Effect of Cr addition on the glass-forming ability, magnetic properties, and corrosion resistance in FeMoGaPCBSi bulk glassy alloys

Baolong Shen, Masahiro Akiba, and Akihisa Inoue

Citation: J. Appl. Phys. **100**, 043523 (2006); doi: 10.1063/1.2335393
View online: http://dx.doi.org/10.1063/1.2335393
View Table of Contents: http://jap.aip.org/resource/1/JAPIAU/v100/i4
Published by the American Institute of Physics.

Effect of Cr addition on the glass-forming ability, magnetic properties, and corrosion resistance in FeMoGaPCBSi bulk glassy alloys

Baolong Shen,[a] Masahiro Akiba, and Akihisa Inoue
Institute for Materials Research, Tohoku University, Sendai 980-8577, Japan

(Received 26 February 2006; accepted 10 June 2006; published online 30 August 2006)

The effect of Cr addition on the glass-forming ability (GFA), the magnetic properties, and corrosion resistance in Fe–Mo–Ga–P–C–B–Si glassy alloys was investigated. In addition to a slight increase of supercooled liquid region from 50 to 55 K, the substitution of a small amount of Fe with Cr was found to be effective for approaching alloy to a eutectic point, resulting in an increase in GFA. By copper mold casting, bulk glassy alloy rods with diameters up to 3 mm were produced. These glassy alloys exhibit a rather high saturation magnetization of 0.84–1.11 T with good soft-magnetic properties, i.e., low coercive force of 2.3–2.9 A/m, and high effective permeability of 13 360–15 960 at 1 kHz under a field of 1 A/m. The passive current density of the glassy alloy rod in 3 mass % NaCl solution decreased significantly from 1×10^{2} to 3×10^{-1} A/m^2 with an increase in Cr content, indicating that the addition of Cr is effective in enhancing the corrosion resistance.
 [DOI: 10.1063/1.2335393]

I. INTRODUCTION

Since bulk glassy alloys (BGAs) consisting only of metallic components in Mg- and lanthanide (Ln)-based systems were synthesized by copper mold casting in the late 1980s,[1,2] a large number of BGAs have been developed. Some BGAs have been used as engineering materials.[3] BGAs have been drawing increasing attention due to their scientific and engineering significance.[4,5] In the case of Fe-based BGAs, since the finding of glass transition before crystallization in Fe-based amorphous alloys, followed by synthesis of Fe–(Al,Ga)–(P,C,B) BGAs,[6,7] many Fe-based ferromagnetic BGA systems have been developed as soft-magnetic materials.[8,9] The development of Fe- and Co-based BGAs with high glass-forming ability (GFA) has attracted increasing interest due to a high potential for applications as structural[10–16] and functional (ferromagnetic)[17–21] materials. The corrosion resistance of Fe-based BGAs have been investigated by Pang *et al.*;[22,23] some Fe-based BGAs with high corrosion resistance were developed in $Fe_{75-x-y}Cr_xMo_yC_{15}B_{10}$ and $Fe_{43}Cr_{16}Mo_{16}(C,B,P)_{25}$ systems. However, those investigations were concentrated on the subject of increasing the corrosion resistance. Large amounts of corrosion-resistant elements Cr and Mo were added, and the Fe content was largely decreased to as low as 30 at. %.[22] As a result, those Fe-based BGAs became nonferromagnetic materials, exhibiting the absence of ferromagnetic properties at room temperature. Therefore, it is necessary to develop Fe-based ferromagnetic BGAs with a high GFA, a high saturation magnetization (I_s), and a good corrosion resistance for applications as ferromagnetic materials in severe environments.

In this study, with the aim of synthesizing Fe-based ferromagnetic BGAs meeting the needs mentioned above, the $Fe_{76}Mo_2Ga_2P_{10}C_4B_4Si_2$ glassy alloy was chosen as a base alloy. This alloy contains a high concentration of Fe, and exhibits a high GFA, that can be cast into bulk glassy alloy rods with diameters up to 2 mm.[24] The effect of Cr addition on the GFA, magnetic properties, and corrosion resistance was investigated, because Cr is effective in enhancing the corrosion resistance in Fe-based BGAs.[22]

II. EXPERIMENT

Multicomponent alloy ingots with compositions of $Fe_{76-x}Cr_xMo_2Ga_2P_{10}C_4B_4Si_2$ ($x=0-6$) were prepared by induction melting. Their compositions are expressed in atomic percentage. The ingots were prepared under a high purified argon atmosphere by using the elements with high purity of Fe (99.9 mass %), Cr (99.9 mass %), Mo (99.9 mass %), Ga (99.9999 mass %), B (99.9 mass %), and Si (99.99 mass %). P and C were alloyed by adding prealloyed Fe-26.5 mass % P and Fe-4.1 mass % C ingots. Those prealloys were also prepared by induction melting and exhibited the purities of 99.9 mass %, respectively. Before induction melting, the chamber of the induction furnace was evacuated to 10^{-3} Pa by a diffusion pump, and then flushed three times with high purified argon gas (99.99 mass %) for obtaining the high purified argon atmosphere. From the master alloy ingots, glassy alloy ribbons with a cross section of 0.02 $\times1$ mm^2 were prepared by meltspinning. Cylindrical rods with diameters up to 4 mm and a length of 40 mm were prepared by injecting the molten alloys contained in a quartz tube into a cylinder-shaped cavity in a copper mold. A high purified argon atmosphere was used during the casting operation, which was the same as that used when preparing the master alloys. Those rods were sectioned by a fine cutter, and the transverse cross sections were examined by x-ray diffraction (XRD) with Cu $K\alpha$ radiation. The thermal stability associated with glass transition temperature (T_g), crystallization temperature (T_x), and supercooled liquid region ($\Delta T_x=T_x-T_g$) was examined by differential scanning calorimetry (DSC) at a heating rate of 0.67 K/s. The melting (T_m) and

[a]Electronic mail: shen@imr.tohoku.ac.jp

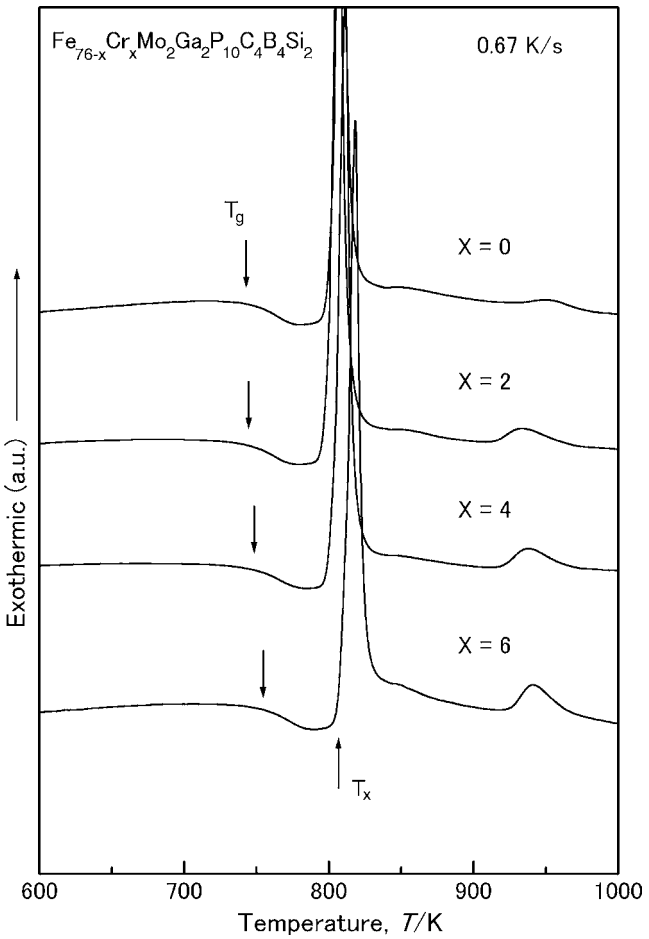

FIG. 1. DSC curves of melt-spun $Fe_{76-x}Cr_xMo_2Ga_2P_{10}C_4B_4Si_2$ (x=0, 2, 4, and 6) glassy alloy ribbons.

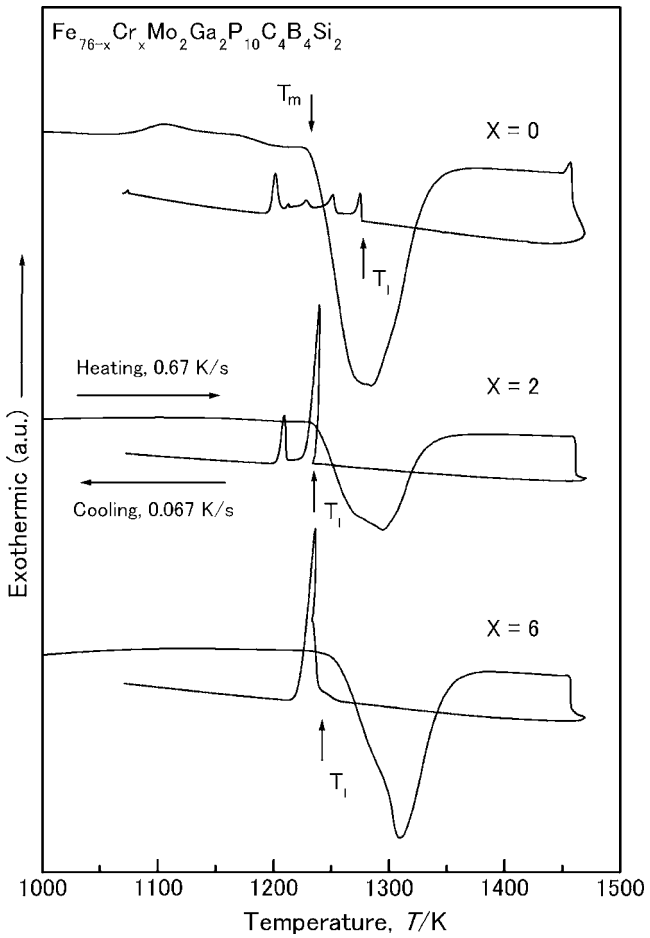

FIG. 2. DTA curves of $Fe_{76-x}Cr_xMo_2Ga_2P_{10}C_4B_4Si_2$ (x=0, 2, and 6) alloys.

liquidus (T_l) temperatures were measured with a differential thermal analyzer (DTA). The heating rate used was 0.67 K/s. To reduce the influence of undercooling during cooling, a cooling rate of 0.067 K/s was used. I_s was measured with a vibrating sample magnetometer under an applied field of 400 kA/m. Coercive force (H_c) was measured with a $B-H$ loop tracer under a field of 800 A/m. Effective permeability (μ_e) at 1 kHz was measured with an impedance analyzer under a field of 1 A/m. Saturation magnetostriction (λ_s) was measured by the three-terminal capacitance method at a sweep speed of 16 kA m^{-1}/s. The corrosion behavior was investigated by electrochemical measurements in 3 mass % NaCl solution open to air at room temperature. The electrochemical measurement was conducted in a three-electrode cell using a platinum counterelectrode and a Ag/AgCl reference electrode. Prior to the electrochemical measurements, the bulk glassy rod samples were degreased in acetone and dried in air. Potentiodynamic polarization curves were measured with a potential sweep rate of 50 mV/min after immersing the samples for 20 min, when the open-circuit potentials had been stabilized.

III. RESULTS

As I_s decreases with decreasing Fe content, in order to obtain a rather high I_s value, the Cr content below 6 at. % was selected in this study. The thermal stability of this alloy system was investigated. Figure 1 shows DSC curves of the $Fe_{76-x}Cr_xMo_2Ga_2P_{10}C_4B_4Si_2$ (x=0, 2, 4, and 6) glassy alloys produced by melt spinning. It is seen that all of the alloys exhibit a distinct glass transition, followed by a supercooled liquid region and then crystallization. The T_g and T_x increase gradually from 738 to 750 K and 788 to 805 K, respectively, with increasing Cr content combined with a slight increase of ΔT_x from 50 to 55 K. The heating and cooling behaviors were investigated using DTA. Figure 2 shows DTA curves of the $Fe_{76-x}Cr_xMo_2Ga_2P_{10}C_4B_4Si_2$ (x=0, 2, and 6) alloys. It is seen that nearly only one endothermic peak appeared in the heating curve for every alloy, although two endothermic peaks overlapped each other and almost became one peak for x=2 and x=6 alloys during heating. This implies that the compositions of this alloy system lie in the vicinity of a eutectic point. On the other hand, from the cooling curves measured at a low cooling rate, it can be seen that T_l decreases from 1277 to 1255 K with increasing Cr content from 0 to 6 at. %. As contrasted with the $Fe_{76}Mo_2Ga_2P_{10}C_4B_4Si_2$ alloy exhibiting several exothermic peaks, the 2 at. % Cr-containing alloy exhibits just two exothermic peaks, and the 6 at. % Cr-containing alloy exhibits only one exothermic peak. In addition, it is also seen from the heating and cooling curves of the Cr-containing alloys that the temperature of T_m is almost the same as that of T_l for each alloy. Therefore, it is considered that the alloy composition approaches a eutectic point with increasing Cr content.

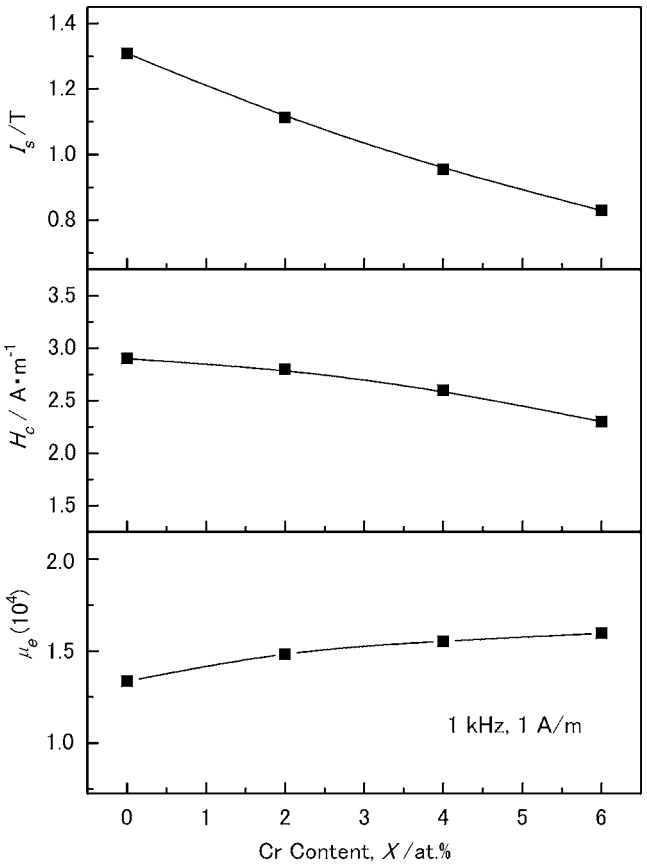

FIG. 3. Changes in I_s, H_c, and μ_e as a function of Cr content for the melt-spun $Fe_{76-x}Cr_xMo_2Ga_2P_{10}C_4B_4Si_2$ (x=0, 2, 4, and 6) glassy alloys.

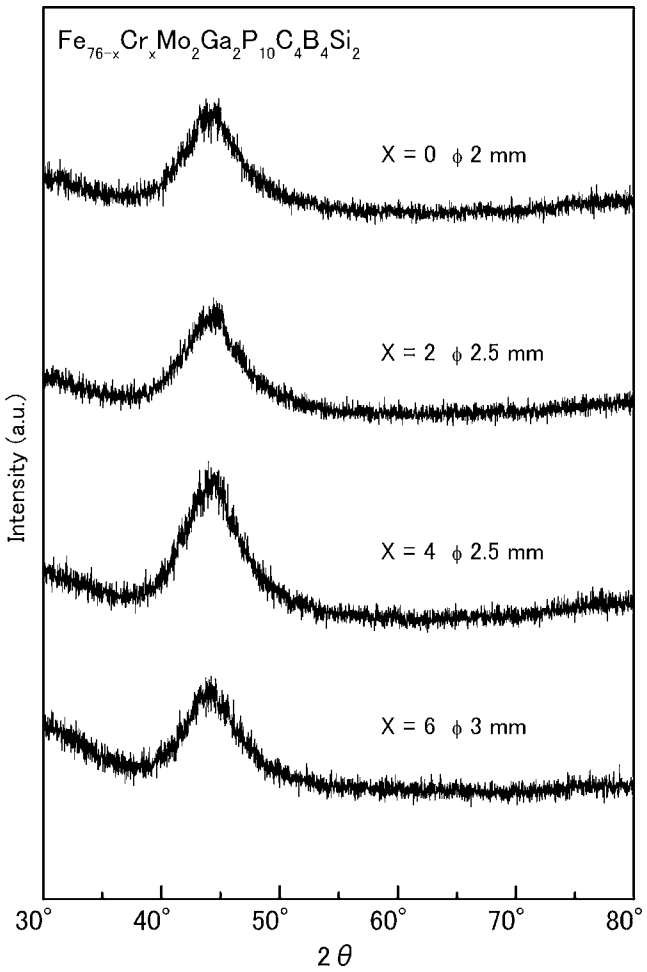

FIG. 4. XRD patterns of the cast $Fe_{76-x}Cr_xMo_2Ga_2P_{10}C_4B_4Si_2$ (x=2, 4, and 6) alloy rods with critical diameters of 2.5, 2.5, and 3 mm, respectively, together with the XRD pattern of the $Fe_{76}Mo_2Ga_2P_{10}C_4B_4Si_2$ glassy alloy rod in a diameter of 2 mm.

The $Fe_{70}Cr_6Mo_2Ga_2P_{10}C_4B_4Si_2$ alloy is the closest to the eutectic point among the alloys. Besides, the reduced glass transition temperatures (T_g/T_l) of those glassy alloys lie in the range of 0.58–0.60.

The magnetic properties were also investigated. Figure 3 shows the changes in I_s, H_c, and μ_e as function of the Cr content for the melt-spun $Fe_{76-x}Cr_xMo_2Ga_2P_{10}C_4B_4Si_2$ (x =0, 2, 4, and 6) glassy alloys. The I_s is 1.31 T for the $Fe_{76}Mo_2Ga_2P_{10}C_4B_4Si_2$ glassy alloy and decreases to 0.84 T by substituting 6 at. % Fe with Cr. The H_c decreases from 2.9 to 2.3 A/m with increasing Cr content, and the μ_e (at 1 kHz, under a field of 1 A/m) increases from 13 360 to 15 960 with increasing Cr content from 0 to 6 at. %. The λ_s was also investigated, but it exhibits almost no distinguishable change with increasing Cr content and exhibits a lower value of 16×10^{-6}. Thus the $Fe_{76-x}Cr_xMo_2Ga_2P_{10}C_4B_4Si_2$ glassy alloys exhibit good soft-magnetic properties.

For the purpose of the applications as soft-magnetic parts, the bulk form is necessary. Based on the results obtained from DSC and DTA measurements, it is concluded that this Fe-based glassy alloy system exhibits a high GFA. We tried to form glassy alloy rods with different diameters up to 4 mm. The glassy alloy rods were produced at all alloy compositions in this system. The critical diameter for formation of a glassy single phase was 2.5 mm for x=2 and 4, respectively, and 3 mm for x=6. Their as-cast surfaces all appear smooth and lustrous. No apparent volume reductions can be recognized on their surfaces, implying that there was no drastic crystallization during the formation of these samples. Figure 4 shows XRD patterns of those cast alloy rods, together with the XRD pattern of the $Fe_{76}Mo_2Ga_2P_{10}C_4B_4Si_2$ glassy alloy rod with a diameter of 2 mm. Only broad peaks without a crystalline peak can be seen in all samples, indicating the formation of a glassy phase with diameters in the range up to 3 mm. The thermal stability of the BGAs was also examined by DSC. Figure 5 shows the DSC curves of the $Fe_{76-x}Cr_xMo_2Ga_2P_{10}C_4B_4Si_2$ (x=2, 4, and 6) glassy alloy rods with diameters up to 3 mm. The DSC curve of the melt-spun glassy alloy ribbon with the same composition as each glassy alloy rod is also shown, respectively, for comparison. No appreciable difference in T_g, ΔT_x, and crystallization process is recognized between the melt-spun ribbon and the BGA for all alloys, indicating the formation of a similar glassy phase. Consequently, both the XRD and DSC measurement results confirmed the formation of the Fe-based BGAs with diameters in the range up to 3 mm.

By using these Fe-based glassy alloy rods, with diameter of 2 mm, we investigated the corrosion resistance by electrochemical measurement. The corrosion behavior of the glassy alloy rod was characterized by potentiodynamic polarization

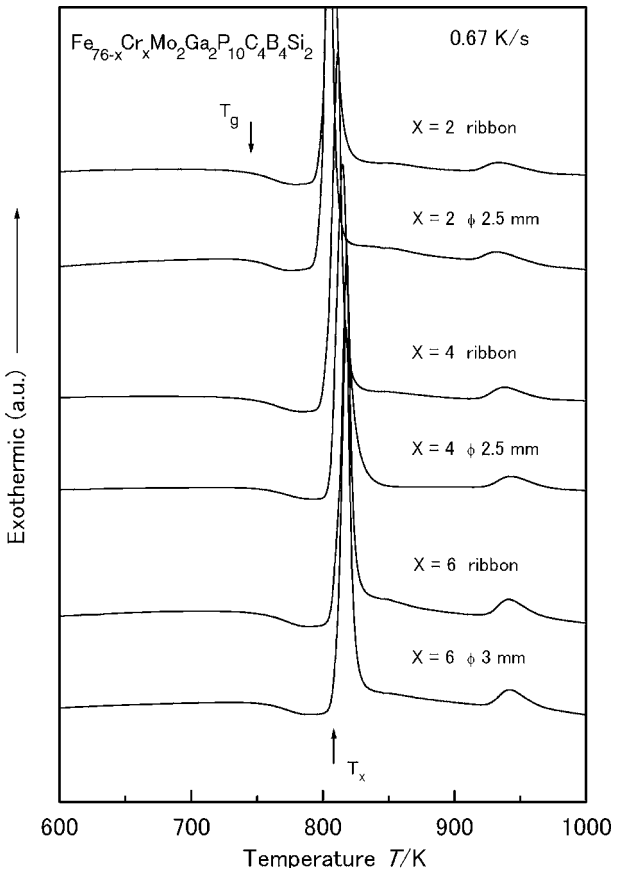

FIG. 5. DSC curves of the $Fe_{76-x}Cr_xMo_2Ga_2P_{10}C_4B_4Si_2$ (x=2, 4, and 6) glassy alloy rods with diameters up to 3 mm. The DSC curve of the melt-spun glassy alloy ribbon with the same composition as every glassy alloy rod is also shown, respectively, for comparison.

in 3 mass % NaCl solution. The anodic polarization curves are shown in Fig. 6. It is seen that the anodic current density decreases significantly with an increase in Cr content. The 4 and 6 at. % Cr-containing glassy alloy rods are spontaneously passivated at a low passive current density of 3×10^{-1} A/m^2, so that the substitution of 4 and 6 at. % Fe with Cr is effective in enhancing the corrosion resistance. Especially for the 6 at. % Cr-containing glassy alloy rod, in addition to a low passive current density, it exhibits the widest passive region before the transpassive dissolution of Cr. This indicates the highest corrosion resistance in comparison with that of the other glassy alloy rod in this Fe-based glassy alloy system. It is therefore concluded that this $Fe_{76-x}Cr_xMo_2Ga_2P_{10}C_4B_4Si_2$ ferromagnetic BGA system simultaneously possesses the high GFA, rather high saturation magnetization, and good soft-magnetic properties, as well as good corrosion resistance.

IV. DISCUSSION

As described above, the substitution of a small amount of Fe with Cr in the $Fe_{76}Mo_2Ga_2P_{10}C_4B_4Si_2$ glassy alloy leads to a significant enhancement of the GFA, the soft-magnetic properties, and corrosion resistance. As shown in Fig. 1, the T_g increases gradually with increasing Cr content up to 4 at. %. It increases faster with further increasing of the Cr content up to 6 at. %. This indicates an increase in the thermal stability of the supercooled liquid. Chen *et al.*[25] have pointed out that electrons could transfer from the metalloid elements such as P, B, and Si to fill the *d* shells in the transition metal elements such as Fe and Cr, and then a *s-d* hybrid bonding is formed. The numbers of 3*d* band electrons in Cr and Fe elements are 5 and 6, respectively; thus the fraction of empty shell of 3*d* band will increase with increasing Cr content. Consequently, it is considered that the *s-d* hybrid bonding nature would become much stronger by adding Cr transition element, because it could supply a large fraction of empty *d* shells. This results in an increase of bonding nature, which is convinced from the mixing enthalpies of the atomic pairs. The enthalpies of mixing for the different atomic pairs are shown in Table I. It is seen that the mixing enthalpies with negative values for the Cr–P, Cr–B, and Cr–Si atomic pairs are larger than those for the Fe–P, Fe–B, and Fe–Si atomic pairs.[26] The mixing enthalpy with

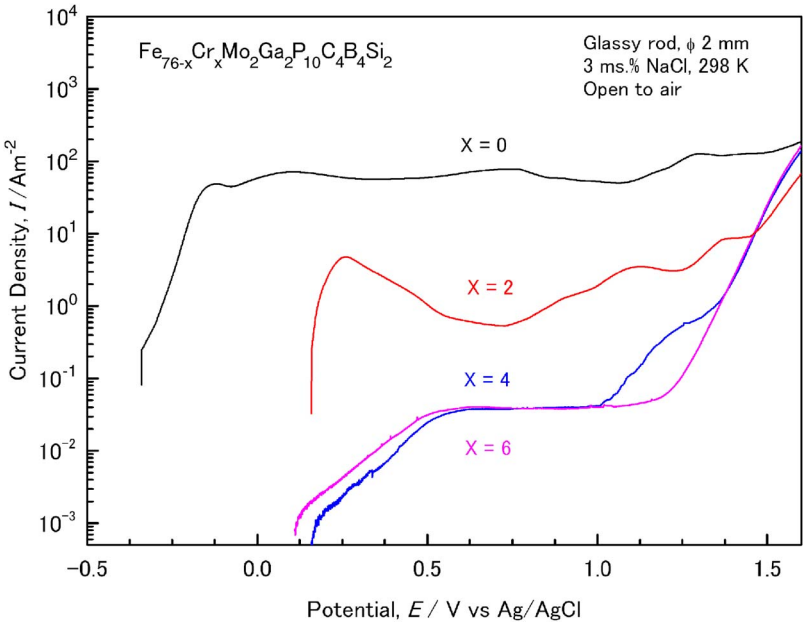

FIG. 6. (Color online) Anodic polarization curves of the $Fe_{76-x}Cr_xMo_2Ga_2P_{10}C_4B_4Si_2$ (x=0, 2, 4, and 6) glassy alloy rods in diameters of 2 mm in 3 mass % NaCl solution open to air at 298 K.

TABLE I. Enthalpies of mixing of constituent elements.

Atomic pair	Enthalpy of mixing (kJ/mol)
Cr–Fe	−1
Cr–Mo	−1
Cr–Ga	−1
Cr–P	−41
Cr–B	−16
Cr–Si	−20
Cr–C	+29
Fe–Mo	−2
Fe–Ga	−2
Fe–P	−31
Fe–B	−11
Fe–Si	−18
Fe–C	+40

positive value for the Cr–C atomic pair is smaller than that of the Fe–C atomic pair.[26] Therefore, the reason for the increase of the thermal stability of the supercooled liquid could be considered as a result of the increase of the bonding nature among the constituent elements by substituting a small amount of Fe with Cr. Otherwise, as shown in the DTA curves, the compositions of this alloy system are located in the vicinity of a eutectic point. It is thus concluded that increasing the stability of the supercooled liquid and approaching alloy to a eutectic point by substituting Fe with Cr lead to the largely increasing GFA. The same result was obtained recently in the Co–Fe–B–Si–Nb BGA system.[21,27]

The behavior that the GFA increases with increasing Cr content is also confirmed from the enhancement of the soft-magnetic properties. It is clearly seen in Fig. 3 that H_c decreases and μ_e increases, respectively, with increasing Cr content. The origin can be attributed to a decrease in internal stress with an increase of GFA. The good corrosion resistance of this Fe–Cr–Mo–Ga–P–C–B–Si BGA system is also considered as a result of the formation of a homogeneous glass single phase. It is known that Cr is one of the most effective alloying elements to provide a high passivating ability for the Fe–Cr-metalloid glassy alloys,[28] as the Cr-rich passive surface films can be formed on the glassy alloy rod in the aggressive solution.[29] In this study, the structurally and chemically homogeneous single-glass phases of the Fe–Cr–Mo–Ga–P–C–B–Si BGA could form a uniform passive film that leads to the significant enhancement of the corrosion resistance.

V. CONCLUSIONS

The substitution of a small amount of Fe with Cr is found to be effective in enhancing the glass-forming ability, soft-magnetic properties, and corrosion resistance. As a result, a ferromagnetic bulk glassy alloy system $Fe_{76-x}Cr_xMo_2Ga_2P_{10}C_4B_4Si_2$ with diameters in the range up to 3 mm was synthesized. This Fe-based ferromagnetic bulk glassy alloy system exhibits a rather high saturation magnetization of 0.84–1.11 T and also a high initial permeability of 13 360–15 960 at 1 kHz under a field of 1 A/m. It showed a good corrosion resistance as well, i.e., spontaneously passivating with a wide passive region and low passive current density of 3×10^{-1} A/m^2 in 3 mass % NaCl solution. The reason for the high-stable supercooled liquid, good soft-magnetic properties, and good corrosion resistance is attributed to the strong bonding nature between the metal and metalloid atoms. This $Fe_{76-x}Cr_xMo_2Ga_2P_{10}C_4B_4Si_2$ ferromagnetic bulk glassy alloy system simultaneously exhibiting high glass-forming ability, good soft-magnetic properties, and good corrosion resistance is promising for future applications as structural and functional materials applied under the severe environmental conditions.

[1] A. Inoue, K. Ohtera, K. Kita, and T. Masumoto, Jpn. J. Appl. Phys., Part 2 **27**, L2248 (1988).
[2] A. Inoue, T. Zhang, and T. Mosumoto, Mater. Trans., JIM **30**, 965 (1989).
[3] A. Inoue, Acta Mater. **48**, 279 (2000).
[4] M. Telford, Mater. Today **7**, 36 (2004).
[5] D. B. Miracle, Nat. Mater. **3**, 697 (2004).
[6] A. Inoue and J. S. Gook, Mater. Trans., JIM **36**, 1180 (1995).
[7] A. Inoue, Y. Shinohara, and J. S. Gook, Mater. Trans., JIM **36**, 1427 (1995).
[8] T. D. Shen and R. B. Schwarz, Appl. Phys. Lett. **75**, 49 (1999).
[9] A. Inoue, A. Takeuchi, and B. L. Shen, Mater. Trans. **42**, 970 (2001).
[10] V. Ponnambalam, S. J. Poon, and G. J. Shiflet, J. Mater. Res. **19**, 1320 (2004).
[11] Z. P. Lu, C. T. Liu, J. R. Thompson, and W. D. Porter, Phys. Rev. Lett. **92**, 245503 (2004).
[12] A. Inoue, B. L. Shen, H. Koshiba, H. Kato, and A. R. Yavari, Acta Mater. **52**, 1631 (2004).
[13] K. Amiya, A. Urata, N. Nishiyama, and A. Inoue, Mater. Trans. **45**, 1214 (2004).
[14] A. Inoue, B. L. Shen, and C. T. Chang, Acta Mater. **52**, 4093 (2004).
[15] S. H. Sheng, C. L. Ma, S. J. Pang, and T. Zhang, Mater. Trans. **46**, 2949 (2005).
[16] B. L. Shen and A. Inoue, J. Phys.: Condens. Matter **17**, 5647 (2005).
[17] P. Pawlik, H. A. Davies, and M. R. J. Gibbs, Appl. Phys. Lett. **83**, 2775 (2003).
[18] W. H. Wang, M. X. Pan, D. Q. Zhao, Y. Hu, and H. Y. Bai, J. Phys.: Condens. Matter **16**, 3719 (2004).
[19] R. B. Schwarz, T. D. Shen, U. Harms, and T. Lillo, J. Magn. Magn. Mater. **283**, 223 (2004).
[20] M. Stoica, S. Roth, J. Eckert, L. Schultz, and M. D. Baro, J. Magn. Magn. Mater. **290–291**, 1480 (2005).
[21] C. T. Chang, B. L. Shen, and A. Inoue, Appl. Phys. Lett. **88**, 011901 (2006).
[22] S. J. Pang, T. Zhang, K. Asami, and A. Inoue, J. Mater. Res. **17**, 701 (2002).
[23] S. J. Pang, T. Zhang, K. Asami, and A. Inoue, Acta Mater. **50**, 489 (2002).
[24] B. L. Shen, M. Akiba, and A. Inoue, Intermetallics (to be published).
[25] H. S. Chen, J. T. Krause, and E. Coleman, J. Non-Cryst. Solids **18**, 157 (1975).
[26] F. R. De Boer, R. Boom, W. C. M. Mattens, A. R. Miedema, and A. K. Niessen, in *Cohesion in Metals*, edited by F. R. De Boer and D. G. Pettifor (North-Holland, Amsterdam, 1989), p. 217.
[27] B. L. Shen, C. T. Chang, T. Kubota, and A. Inoue, J. Appl. Phys. **100**, 013505 (2006).
[28] K. Asami, K. Kawashima, and K. Hashimoto, Mater. Sci. Eng. **99**, 475 (1988).
[29] S. J. Pang, T. Zhang, K. Asami, and A. Inoue, Corros. Sci. **44**, 1847 (2002).